J Mol Model (2013) 19:811–824
DOI 10.1007/s00894-012-1597-7

ORIGINAL PAPER

A three-layer ONIOM model for the outside binding of cationic porphyrins and nucleotide pair DNA

Gloria I. Cárdenas-Jirón · Luis Cortez-Santibañez

Received: 29 February 2012 / Accepted: 19 September 2012 / Published online: 11 October 2012

Abstract In this work we investigated the outside binding mode between a cationic porphyrin and a nucleotide pair of DNA, adenine-thymine and guanine-cytosine, in a supramolecular assembly. We used two structural models (semi-extended, extended) that differ in the size of porphyrin, two kinds of theoretical methods: a three layer ONIOM (B3LYP/6-31G(d)/PM3/UFF), and DFT B3LYP/6-31G(d,p), and three cationic porphyrins. ONIOM method was first tested on the semi-extended model that was calculated in four environments: gas phase, solution phase using an explicit solvent model (H_2O), in the presence of a sodium cation (Na^+) and in both (H_2O + Na^+). From interaction energy results, we found that the affinity of the cationic substituent by the adenine nucleotide is favored upon the thymine nucleotide. The extended model that considers the whole porphyrin was applied in the gas phase to the four nucleotides. All the cationic porphyrins showed affinity by the nucleotides in the order adenine > guanine > thymine > cytosine. The interaction energy values for outside binding showed a strong porphyrin-nucleotide interaction (≈-90 kcal mol^{-1}), that slightly varies between the nucleotides suggesting that this kind of cationic porphyrin has a little selectivity for some of them. We also found that the effect of the nature of the cationic substituent (chain length) in the porphyrin on the outside binding is small (≈2–13 kcal mol^{-1}). Coherence between the results showed that ONIOM is a useful tool to get a reasonable molecular geometry to be used as a starting point in calculations of density functional theory.

Keywords Cationic porphyrin · DNA · ONIOM · Outside binding

Introduction

Over the last decades there was a great interest for studying the porphyrins because they can interact with DNA or oligonucleotides and act as photosensitizers in photodynamic therapy (PDT) [1–11]. Fiel et al. showed for the first time the interaction of a cationic porphyrin TMPyP (*meso*-tetrakis (4-N-methylpyridiniumyl) porphyrin) and a double strand DNA, and proposed three binding modes for this interaction: intercalation, outside binding with self-stacking and outside binding without self-stacking (groove) [12]. Several techniques have been used that give evidence of the porphyrin and DNA interaction such as UV-visible absorption spectroscopy, circular dichroism, electron paramagnetic resonance, nuclear magnetic resonance, fluorescence spectroscopy, viscosity and thermal denaturation [8–11, 13, 14].

TMPyP is one of the more widely studied cationic porphyrin [3, 12, 15–17], and metal derivatives of TMPyP have also been proved as binders to DNA. Metal derivatives of TMPyP with no axial ligand having Au(III), Ni(II), Pt(II) and Cu(II) possess a planar geometry favorable to intercalate at cytosine-guanine sites [18–20], while those with axial ligands having Zn(II), Fe(II), Co(III), Mn(II) and V(IV) bind to the outside of DNA without self-stacking in adenine thymine rich sequences [21]. Other kinds of cationic porphyrins have also been investigated for a binding with DNA sequences and it has been found that depending on their structures they prefer certain sequences. TMAP (meso-

Electronic supplementary material The online version of this article (doi:10.1007/s00894-012-1597-7) contains supplementary material, which is available to authorized users.

G. I. Cárdenas-Jirón (✉) · L. Cortez-Santibañez
Theoretical Chemistry Laboratory, Faculty of Chemistry and Biology, University of Santiago de Chile (USACH),
Casilla 40, Correo 33,
Santiago, Chile
e-mail: gloria.cardenas@usach.cl

tetrakis(N-trimethylanilinium-4-yl)porphyrin) that has a non planar substituent binds to calf thymus DNA in an outside binding with self stacking [16], and porphyrins with long substituent on the meso aromatic rings such as TθpyP (meso- tetrakis [4-N-(3-trimethylammoniumpropyl) pyridyl] porphyrin) intercalated into guanine cytosine base pairs. A similar porphyrin without pyridinium groups such as TθOPP (meso-tetrakis [4-[3-trimethylaminopropyl)oxy] phenyl]- porphyrin) self stacked along the DNA backbone [22, 23]. Studies on understanding the binding interactions of cationic porphyrins with B-form DNA have shown that the base composition and not the sequence determine the mode of binding [3]. This has been proved in TθF4TAP (meso-tetrakis [2,3,5,6-tetrafluoro-4-(2-trimethylammoniumethylamine) phenyl] porphyrin) which binds at both adenine-thymine and cytosine-guanine rich sequences showing that the binding is strongly affected by the composition of the base pair [24]. For dicationic pyridium porphyrins (12 molecules) it has been shown that the affinity for DNA and the binding mode could be modulated by the position of the positive charge and the steric hindrance, and the photocleaving ability of DNA to be affected [25].

The quantum chemistry methods can investigate in detail at a molecular level the composition of the base pair and the nature of the substituent in the porphyrin and also provide enough theoretical bases for predicting the binding mode that a porphyrin will have with DNA. These results could be useful for chemists doing experiments to complement their studies.

In this work, our purpose is to investigate at a molecular level the outside binding between a cationic porphyrin (Fig. 1) and a nucleotide pair (adenine-thymine, cytosine-guanine) (Fig. 2) forming a supramolecular assembly, this means that we analyzed the factors (molecular environment, substituent nature) affecting that interaction, the stability of this one and the selectivity of the cationic porphyrin toward the nitrogenous base, and the consequences of such interaction (molecular structure, charge transfer).

Computational details

Structural models

This study was done in a systematic form, so we used two structural models for the supramolecular assemblies which present a difference in their sizes, *semi-extended* and *extended model*, and are shown in Fig. 3 for the pair adenine-thymine. A similar extended model was used for the pair guanine-cytosine. All the models are calculated in the gas phase, but in order to investigate a more realistic picture the semi-extended model is also calculated in the solution phase using a solvent explicit model (four water molecules), in the presence of a sodium cation (Na^+) and taking into account both environments water and sodium cation ($4H_2O + Na^+$).

The semi-extended model utilizes a three layer ONIOM model (Fig. 3a), developed by Morokuma et al. [26–28] ONIOM is a general hybrid method, which can combine

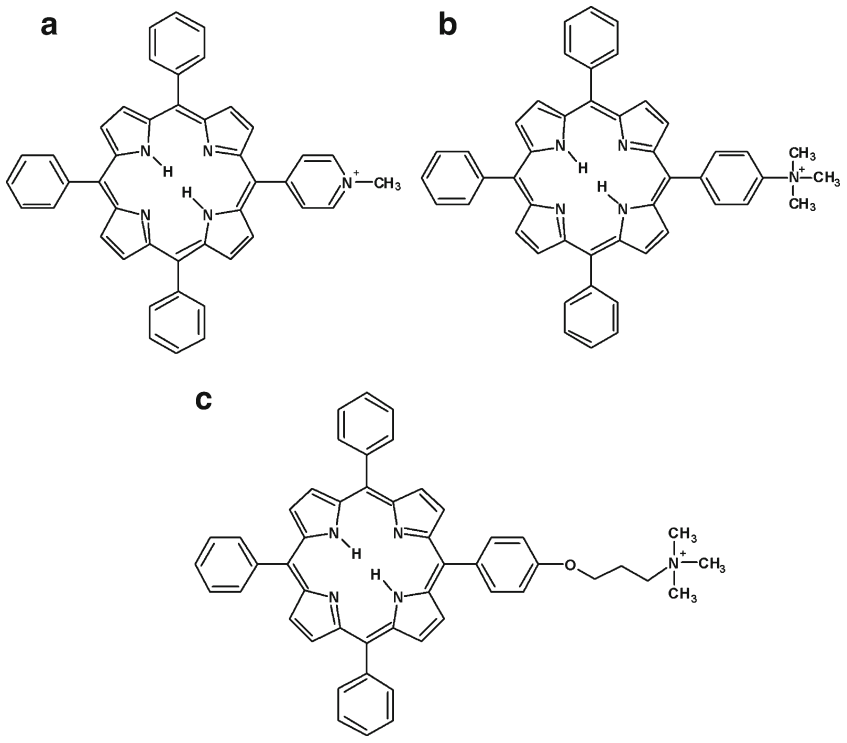

Fig. 1 View of the molecular structure of cationic porphyrins: (**a**) $MmPyP^+$: Meso-mono(N-methylpyridiniumyl)triphenyl-porphyrin; (**b**) MmAP+: Meso-mono(trimethylaniliniumyl)triphenylporphyrin; (**c**) MONPP+: Meso-mono[(3-trimethylamino-propyl)oxiphenyl] triphenylporphyrin

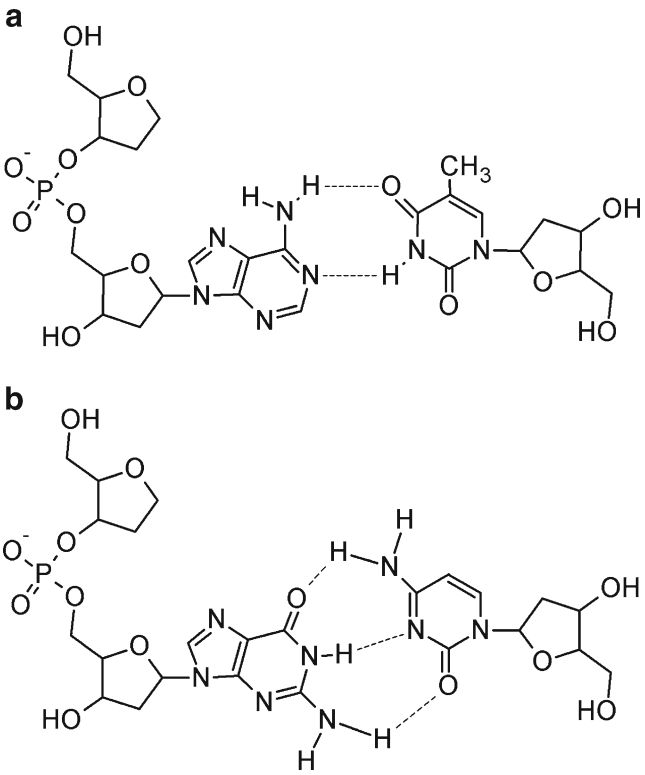

Fig. 2 Structural model of a pair of nucleotide: (**a**) adenine (left)-thymine (right); (**b**) guanine (left)-cytosine (right)

quantum mechanics (QM) as well as molecular mechanics (MM) methods, and it is reported to be an efficient tool for accurately calculating chemical interactions in large systems [29–34].

The semi-extended model is composed of mPy^+ (N-methyl pyridyl cation) interacting with PO_4^- (phosphate group), the latter being bonded to two ribose (R) units, trying to simulate the environment that this group would have in a DNA strand. We used two nucleotides with the adenine (A) and thymine (T) base pair, where only one phosphate group was considered, which belongs to the concern region interacting with mPy^+ (see Fig. 3). This assembly is calculated in the gas phase (**1**), and in different environments, in the solution phase with explicit solvent (water) (**2**), in the presence of Na^+ (**3**) and in both H_2O + Na^+ (**4**). In an arbitrary form we choose four water molecules distributed along the region where mPy^+ and PO_4^- are localized, with the aim to study the effect that they produce on the outside binding. The idea of using four environments is, on the first hand, to do a modeling closer to the real environment that DNA has and, on a second hand, is to carry out a systematic study that shows the trend of behavior for the outside binding.

As is illustrated in Fig. 3a, the semi-extended model is divided in three layers, following the ONIOM nomenclature: (a) high layer; (b) medium layer and (c) low layer. The high layer takes into account the critical part of the interacting system ($mPy^+\cdots PO_4^-$) and constitutes the model system that is calculated employing density functional theory (DFT) with B3LYP/6-31G(d) (red in Fig. 3a) [35–37]. The medium layer corresponds to the adenine thymine base pair (A···T) and is calculated also with quantum mechanics but at a lower level than DFT, in this case we used a semiempirical method PM3 [38] (green in Fig. 3a). This method was used to reasonably treat the hydrogen bonding between adenine and thymine, and has been shown to be enough to describe this kind of interaction [39, 40].

The ribose units have been treated with MM using the UFF force field [41] (black in Fig. 3a) because it is expected that these units do not participate in the interaction with mPy^+. Both the water (H_2O) and sodium cation (Na^+) are calculated as high layer. All the assemblies described above for the semi-extended model (gas phase, H_2O and/or Na^+)

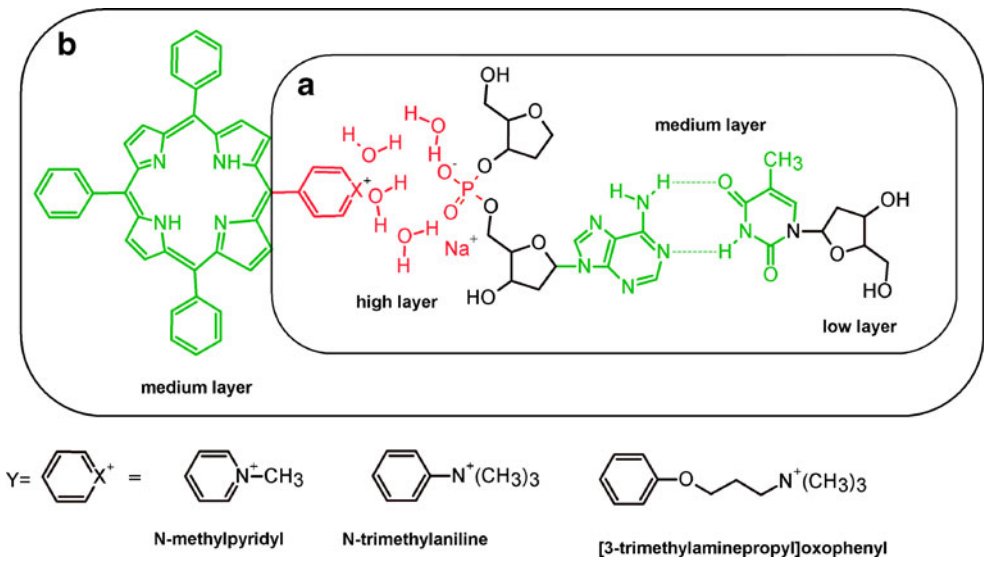

Fig. 3 Structural models for the interaction of a cationic porphyrin with a nucleotide pair of adenine-thymine: (**a**) semi-extended; (**b**) extended

are fully optimized without any symmetry restriction at the levels of theory already mentioned using the ONIOM methodology, it means B3LYP/6-31G(d)/PM3/UFF for high/medium/low layers, respectively.

For more clarity we will use throughout the article an abbreviated nomenclature; R: ribose ring; A: adenine; T: thymine. Besides to study the interaction $mPy^+\cdots PO_4^-$ by the side of adenine ($mPy^+\cdots PO_4^-$ $R_2A\cdots TR$), we also investigated the interaction by the side of thymine denoted by $RA\cdots TR_2PO_4^-\cdots mPy^+$, where the same three layers ONIOM model is applied. The numeration used for the latter assemblies are denoted by a prime **1′**, **2′**, **3′**and **4′**. The calculations obtained from both kinds of interactions will help to understand the selectivity of mPy^+ toward the base (adenine, thymine), that is the affinity that the cation mPy^+ has with the different nucleotides. This is the reason why we used the environments localized only in the region where we will calculate the outside binding.

With the aim of having a more realistic picture of the interaction porphyrin (P)···nucleotide DNA, the extended model (Fig. 3b) takes into account the whole mono cationic porphyrin (PY) (Fig. 1) instead of only the N-methyl pyridyl cation. Here Y corresponds to the cationic substituent bonded to the porphyrin. In this case we also applied a three layer ONIOM model, for the region of interest ($Y\cdots PO_4^-$) we used B3LYP/6-31G(d), the semiempirical PM3 method for the base pair and the porphyrin, and molecular mechanics (UFF) for the ribose units. Due to the increased size of the extended model, the inclusion of an explicit solvent, as was done for the semi-extended one, was not possible and the study was performed in the gas phase. The use of a continuum solvent model is not available for ONIOM calculations in the computational package available in this work (Gaussian03) [32].

We studied three monocationic porphyrins using the extended model that present a difference in the cationic substituent Y (Fig. 1), these are the assemblies **5-7** for the interaction by adenine nucleotide and **5′-7′** by thymine nucleotide. These porphyrins with tetra cationic substitution have been investigated previously at an experimental level and they preferably bind to adenine-thymine rich sequences [12, 16, 22, 23]. We investigated how the chain length in X^+ affects the interaction with PO_4^-. As was done for the semi-extended model, the assemblies corresponding to the extended model are fully optimized without any symmetry restriction at the levels of calculation mentioned above using the ONIOM methodology, that is B3LYP/6-31G(d)/PM3/UFF for high/medium/low layers, respectively.

The same methodology used for AT is also applied to guanine cytosine (GC) nucleotides and the three porphyrins, and the interaction is studied for both by guanine side (**8-10**) or cytosine side (**8′-10′**).

For each optimized assembly as for the semi-extended model as for the extended model a calculation of the vibrational frequency is done, and it is verified that all assemblies have positive values for the frequencies confirming that they correspond to structures of minimum energy.

Interaction energies

The interaction that mPy^+ (or PY) presents with the rest of the structural model (semi-extended and extended) was evaluated by determining the energy associated to that interaction. For the semi-extended and extended models, we determined two types of interaction, one of them corresponding to the outside binding of mPy^+ (or PY) and the other one associated to the interaction between the base pair. The outside binding is calculated on the adenine side and the thymine side for both structural models, and on the guanine side and the cytosine side only for the extended model. For each one we calculated the energy due to the hydrogen bonding between the bases, so in total we determine four interaction values for each supramolecular assembly in each one of the molecular environments (gas phase, $4H_2O$ and/or Na^+).

For the semi-extended model, the interaction of N-methyl pyridyl ring with the nucleotide pair by the adenine side calculated in the gas phase is given by:

$$E_1 = E(mPy^+\cdots PO_4^-R_2A\cdots TR) - \left[E(mPy^+) + E(PO_4^-R_2A\cdots TR)\right]. \quad (1)$$

For the other environments ($4H_2O$, Na^+, $4H_2O$ + Na^+) similar equations are used but always taking into account the interaction of the assembly with the mPy^+:

$$E_2 = E(mPy^+\cdots 4H_2O\cdots PO_4^-R_2A\cdots TR) - \left[E(mPy^+) + E(4H_2O\cdots PO_4^-R_2A\cdots TR)\right], \quad (2)$$

$$E_3 = E(mPy^+\cdots Na^+\cdots PO_4^-R_2A\cdots TR) - [E(mPy^+) + E(Na^+\cdots PO_4^-R_2A\cdots TR)], \quad (3)$$

$$E_4 = E(mPy^+\cdots 4H_2O\cdots Na^+\cdots PO_4^-R_2A\cdots TR) - [E(mPy^+) + E(4H_2O\cdots Na^+\cdots PO_4^-R_2A\cdots TR)]. \quad (4)$$

The corresponding interactions on the side of thymine are calculated in a similar form to adenine, just taking into account that the assembly has changed. The calculation in the gas phase is given by:

$$E_{1'} = E(RA\cdots TR_2PO_4^-\cdots mPy^+) - [E(mPy^+) + E(RA\cdots TR_2PO_4^-)], \quad (5)$$

and in the other molecular environments $4H_2O$, Na^+ and ($4H_2O + Na^+$) is done in a similar form to E_2-E_4 ($E_{2'}$-$E_{4'}$).

In the case of the extended model (Fig. 1), we calculated the interaction energy by the adenine side (E_5-E_7), thymine side ($E_{5'}$-$E_{7'}$), guanine side (E_8-E_{10}) and cytosine side ($E_{8'}$, $E_{10'}$). As an example, we show the expression used for the adenine and thymine sides:

$$E_5 = E(PY \cdots PO_4^- R_2A \cdots TR) - [E(PY) + E(PO_4^- R_2A \cdots TR)], \quad (6)$$

$$E_{5'} = E(RA \cdots TR_2PO_4^- \cdots PY) - [E(PY) + E(RA \cdots TR_2PO_4^-)]. \quad (7)$$

Natural population analysis (NPA) based on the natural atomic orbital (NAO) scheme [42, 43] was done by means of single point calculations over the ONIOM optimized geometries at the level of theory B3LYP/6-31G(d,p). All calculations were carried out with the quantum chemistry package Gaussian03 Rev. E.01 [44].

Results and discussion

Semi-extended model

We investigated the interaction of the N-methylpyridyl cation with a phosphate anion (PO_4^-) linked to a nucleotide pair of DNA (Fig. 3). Note that PO_4^- is bonded to two ribose rings for simulating in a more realistic form the molecular environments that this group has in the double strand DNA. In order to reduce the complexity of the whole structural model, this part of the strand is used only in one side of the nucleotide where mPy^+ is found.

The semi-extended model is a simple model (Fig. 3), where we only consider the cationic substituent of the porphyrin, in order to reduce the size of the latter. This model is used to study the effect of the nucleotide (adenine, thymine) on the outside binding ($mPy^+ \cdots PO_4$), and also the effect of the environment given by water and sodium cation on that interaction. The aqueous environment is chosen because it corresponds by default to the natural medium of DNA, and the sodium cation is included in the study because it represents the ionic force that is present around of DNA.

Figures 4 and 5 show the optimized molecular structures obtained with ONIOM methodology calculated for the interaction $mPy^+ \cdots PO_4^-$ with the adenine nucleotide and the thymine nucleotide, respectively. As is usual in a three layer ONIOM model, the ball and stick model in these figures represents the high layer that is calculated at the density functional theory and corresponds to the interest region, the

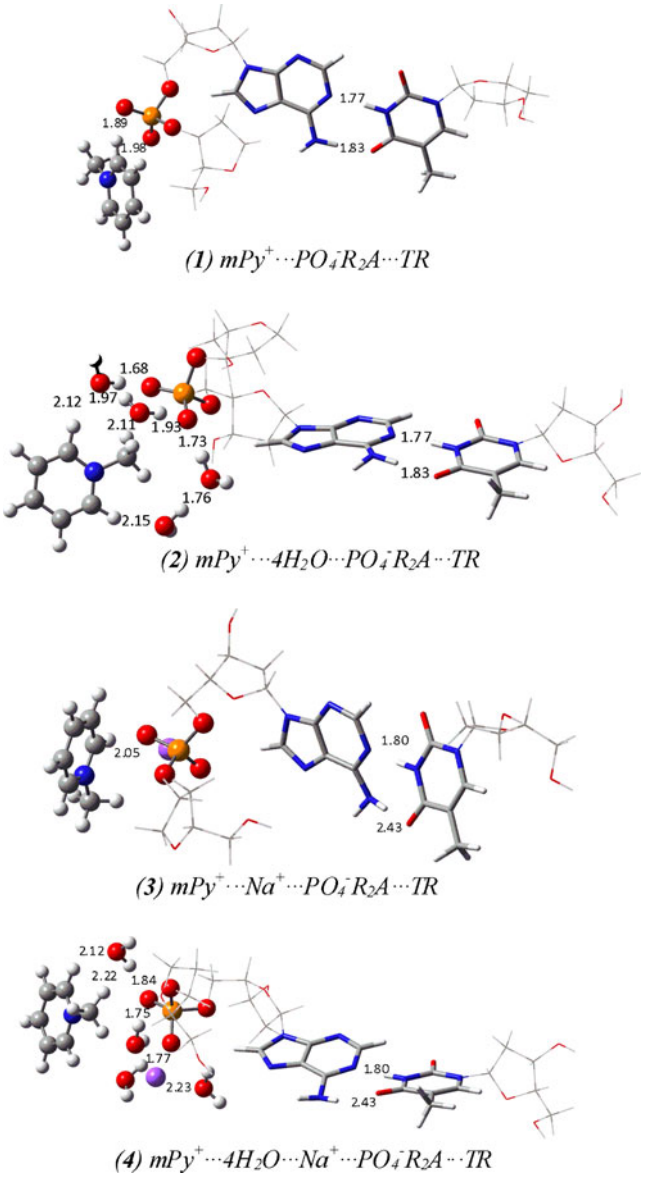

Fig. 4 Optimized molecular assemblies obtained by ONIOM methodology for the semi-extended model where the outside binding of mPy^+ is by the adenine nucleotide. All distances shown are in angstroms

interaction $mPy^+ \cdots PO_4^-$. The tube model represents the medium layer calculated with the semiempirical PM3 method and in this case corresponds to the interaction between the base pairs. The wireframe model represents the low layer that is expected not to change by the outside binding and is calculated with molecular mechanics.

Overall, we can see in both figures that several hydrogen bonds are formed between mPy^+ and PO_4^-, and the inclusion of environments (H_2O, Na^+) has an effect on this bonding due to the formation of new H-bonds. For the interaction by the adenine side (Fig. 4), in **1** two strong H-bonds between the hydrogen atoms of mPy^+ and the oxygen atoms of PO_4^- are formed, at 1.89 and 1.98 Å. The inclusion of water

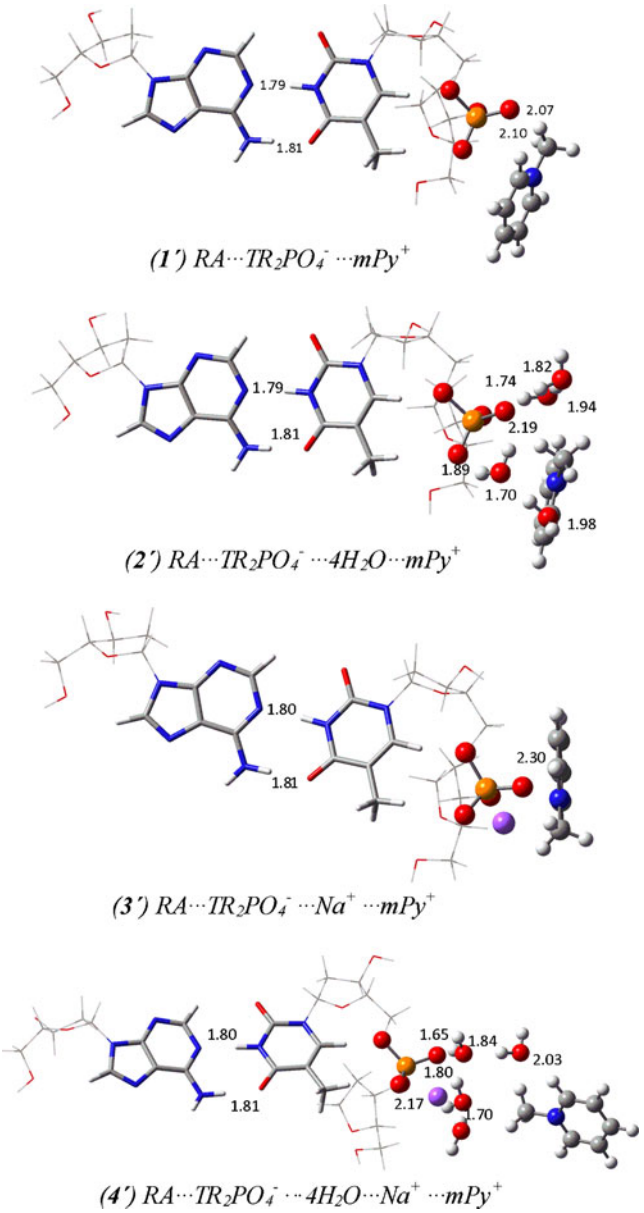

Fig. 5 Optimized molecular assemblies obtained by ONIOM methodology for the semi-extended model where the outside binding of mPy^+ is by the thymine nucleotide. All distances shown are in angstroms

molecules (four), **2**, weakens the attraction of both PO_4^- and mPy^+ ions shifting the latter to larger distances, resulting in the formation of H-bonds between the species $mPy^+\cdots H_2O$ (three), $PO_4^-\cdots H_2O$ (three) and $H_2O\cdots H_2O$ (two). When the sodium cation is incorporated to **1** generating the assembly **3**, one H-bond is formed between mPy^+ and PO_4^- at distances a little larger (2.05 Å) than **1** (1.89 and 1.98 Å), indicating that the inclusion of Na^+ produces a decrease in the force of the interaction $mPy^+\cdots PO_4^-$. The latter can be explained for a competence between both positively charged species, mPy^+ and Na^+. If both H_2O and Na^+ are included to the assembly **1** generating **4** the amount of H-bonds decreases with respect to **2**, two for the interaction $mPy^+\cdots H_2O$ (2.12 and 2.22 Å) and three for the interaction $PO_4^-\cdots H_2O$ (1.75, 1.77 and 1.84 Å).

On the other hand, we analyzed the interaction between the adenine and thymine bases which present two strong H-bonds (N···H, H···O) (1.7–1.8 Å) when mPy^+ is approached. The inclusion of the aqueous solvent (four H_2O molecules) (**2**) does not produce any change in the hydrogen bonding, but Na^+ produces a longer distance H···O (2.43 Å) in **3** and **4**, indicating a weaker interaction between the base pair.

The interaction of $mPy^+\cdots PO_4^-$ by the thymine nucleotide (**1′**) produces larger values (2.07 and 2.10 Å) of the H-bonds with respect to **1** (1.89 and 1.98 Å) indicating that although the interaction between the species occurs this is weaker. The inclusion of water molecules leading to **2′** generates as expected a similar behavior as that in **2**, two H-bonds for each interaction, $mPy^+\cdots H_2O$, $PO_4^-\cdots H_2O$ and $H_2O\cdots H_2O$, but in this case one H-bond for the interaction $mPy^+\cdots PO_4^-$ at a distance of 2.19 Å, which is larger than 2.07 Å of **1′**. The assembly **3′** shows one H-bond for $mPy^+\cdots PO_4^-$ at a value of 2.30 Å, which is longer than 2.05 Å in **3**. Finally the optimized assembly with both H_2O and Na^+ (**4′**) has one H-bond for the interaction $mPy^+\cdots H_2O$ (2.03 Å), two for the interaction $PO_4^-\cdots H_2O$ (1.65 and 1.80 Å) and two for the interaction $H_2O\cdots H_2O$ (1.70 and 1.84 Å). In comparison with **4**, the assembly **4′** has fewer H-bonds although they are shorter and in consequence stronger than the former.

In relation to the hydrogen bonding produced between the base pair (1′-4′), we found that practically they do not undergo a modification (1.79 and 1.81 Å) by the change produced in the region of the phosphate anion and the N-methylpyridyl cation (Fig. 5).

In summary, we found that the interaction $mPy^+\cdots PO_4^-$ in **1** and **3** occurs at smaller distances when it is produced by the adenine nucleotide suggesting that mPy^+ is selective to the nitrogenous base. Besides, we also observed that this fact is correlated with the results obtained for the hydrogen bonding between the base pair, the initial values of $r_{N\cdots H}$= 1.77 Å and $r_{O\cdots H}$=1.83 Å for **1** change by the inclusion of Na^+ in **3** (1.80 Å and 2.43 Å) indicating a decrease in the interaction between the bases. The results obtained for the interaction by the thymine nucleotide show a constant value for the hydrogen bonding between the base pair, which can be understood because of the smaller effect that provokes the interaction $mPy^+\cdots PO_4^-$ calculated in their different environments on the base pair.

In order to quantify the affinity between mPy^+ and PO_4^-, the interaction energies were calculated for the gas phase (E_1) and for the other three environments (E_2, E_3, E_4). Using the ONIOM optimized geometry that was previously discussed; we calculated these energies at the level of calculation used in ONIOM (B3LYP/PM3/UFF). As a comparison, we also calculated the interaction energies at the density

functional level (B3LYP/6-31G(d,p)) for the whole assembly using the optimized ONIOM geometries, and the results obtained are shown in Table 1. We also calculated the interaction between the base pair denoted by A···T.

First, we analyze the outside binding, all the interaction energies have negative values indicating that the interaction between mPy^+ and the nucleotide pair is favored.

For the three layers ONIOM we found that the interaction energy for the assembly with water increases with respect to the gas phase in 15 kcal mol^{-1} for adenine side and in 1 kcal mol^{-1} for thymine side. A similar result is found when Na^+ is included, the interaction energy also increases but in this case the effect is larger, 79 and 77 kcal mol^{-1} by adenine (**3**) and thymine (**3´**) side, respectively. In **2** and **2`** the mPy^+ interacts with a hydrated phosphate group where the four water molecules avoid the free approach of the positive charge leading to a lower affinity $mPy^+\cdots PO_4^-$ than in the gas phase. The effect produced by sodium cation is similar in the sense that it weakens the interaction $mPy^+\cdots PO_4^-$ but is larger because of the size and affinity of Na^+ by PO_4^-. Certainly the presence of both H_2O and Na^+ shows an increased effect.

The results obtained with B3LYP follow a similar trend as those obtained with three layers ONIOM. The presence of Na^+ produces an unstabilization of 64 kcal mol^{-1} in **3** and 62 kcal mol^{-1} in **3´** with respect to the gas phase (**1**, **1´**), and the inclusion of both Na^+ and H_2O leads to an increase of 55 kcal mol^{-1} for **4** and 70 kcal mol^{-1} for **4´**. However, when only four water molecules are added, the interaction energy for the outside binding slightly decreases (1 kcal mol^{-1} in **2**; 2 kcal mol^{-1} in **2´**). Clearly the interaction $mPy^+\cdots PO_4^-$ is weaker in the presence of different environments for the intermolecular interactions produced but the results show that cationic species like mPy^+ develop an interaction with the phosphate anion of the nucleotide.

One aspect to be highlighted corresponds to the fact that in all the cases (with exception of **4**) the ONIOM method provides lower interaction energies than B3LYP. This is relevant taking into account that the former takes less computational time than the latter. Overall, we found that the effect of the presence of water is ≈ 1–15 kcal mol^{-1} and the effect of the presence of sodium cation is ≈ 60–80 kcal mol^{-1}, these differences are very clear and could be understood in terms of the nature of the interaction that they govern, hydrogen bonding and electrostatic, respectively.

Another relevant aspect of this work is that from both methods of calculation, ONIOM, B3LYP, we found that always the interaction by adenine side generates lower interaction energy than by thymine side, indicating that mPy^+ has a larger affinity for the former. For the three layers ONIOM, the interaction by adenine nucleotide is more stable in≈13–16 kcal mol^{-1} than by the thymine nucleotide, depending on the environment. In the case of B3LYP the

Table 1 Interaction energies E_{int} (kcal mol^{-1}) for the outside binding of mPy^+ with the nucleotide pair and for the *A···T* bases in the assemblies of the semi-extended model

	Outside binding			Outside binding	
Interaction by adenine nucleotide	E_{int} three layers ONIOM	E_{int} B3LYP[a]	Interaction by thymine nucleotide	E_{int} three layers ONIOM	E_{int} B3LYP[a]
1: $mPy^+\cdots PO_4^-R_2A\cdots TR$	-105.26	-86.1	***1´***: $RA\cdots TR_2\ PO_4^-\ mPy^+$	-91.90	-78.1
2: $mPy^+\cdots 4H_2O\ PO_4^-R_2A\cdots TR$	-90.18	-87.3	***2´***: $RA\cdots TR_2\ PO_4^-\ 4H_2O\ mPy^+$	-90.20	-80.4
3: $mPy^+\cdots Na^+\ PO_4^-R_2A\cdots TR$	-25.73	-22.3	***3´***: $RA\cdots TR_2\ PO_4^-\ Na^+\ mPy^+$	-14.89	-16.3
4: $mPy^+\cdots 4H_2O\ Na^+\ PO_4^-R_2A\cdots TR$	-25.30	-31.3	***4´***: $RA\cdots TR_2\ PO_4^-\ 4H_2O\ Na^+\ mPy^+$	-9.40	-8.0
	A···T			*A···T*	
Interaction by adenine nucleotide	E_{int} three layers ONIOM	$E_{int.}$ B3LYP[a]	Interaction by thymine nucleotide	E_{int} three layers ONIOM	E_{int} B3LYP[a]
$PO_4^-R_2A\cdots TR$	-4.28	-13.3	$RA\cdots TR_2\ PO_4^-$	-4.79	-15.2
1: $mPy+\cdots PO_4^-R_2A\cdots TR$	-5.71	-15.9	***1´:*** $RA\cdots TR_2\ PO_4^-\ mPy+$	-5.88	-14.1
2: $mPy+\cdots 4H_2O\ PO_4^-R_2A\cdots TR$	-5.63	-15.8	***2´:*** $RA\cdots TR_2\ PO_4^-\ 4H_2O\ mPy+$	-5.37	-15.5
3: $mPy+\cdots Na+\ PO_4^-R_2A\cdots TR$	-4.77	-14.6	***3´:*** $RA\cdots TR_2\ PO_4^-\ Na+\ mPy+$	-5.41	-18.1
4 : $mPy+\cdots 4H_2O\ Na+\ PO_4^-R_2A\cdots TR$	-4.72	-14.9	***4´:*** $RA\cdots TR_2\ PO_4^-\ 4H_2O\ Na+\ mPy+$	-5.19	-16.1

[a] basis set: 6–31 G(d,p)

higher stability of mPy^+ by the adenine side is ≈ 6–23 kcal mol^{-1}. Based on these results one can say that there exists a selectivity degree between the nucleotides by the outside binding.

On the other hand, we also investigate the interaction between the bases adenine-thymine (A···T) that corresponds to hydrogen bonding, and the energy associated to this interaction for each assembly (**1-4**, **1′-4′**) is presented in Table 1. We also included the value of the nucleotide pair without mPy^+ to see its effect on the interaction energy. Note that the nucleotide pair differs in the number of ribose rings and the presence of phosphate group, hence the energy values are different (-4.28, -4.79 kcal mol^{-1}). For both methods, with exception of **1′** in B3LYP, the results indicate that the binding energies between the bases are more negative when mPy^+ interacts with the nucleotides with respect to the isolated nucleotide pair (ONIOM: -4.28, -4.79; B3LYP: -13.3, -15.2 kcal mol^{-1}). Then mPy^+ stabilizes the interaction A···T. By the contrary to the obtained results for the outside binding, the A···T interaction energies calculated with ONIOM are higher than B3LYP, which can be explained due to that the interaction region between bases has been described by a semiempirical method PM3, that is an approximated method that considers only the valence electrons in the calculation instead of the full electrons (valence and core). The values predicted by ONIOM (≈ 5 kcal mol^{-1}) are underestimated considering that two hydrogen bonds are formed between adenine and thymine, which indicates that PM3 does not provide reliable values for that interaction. However, B3LYP predicts A···T interaction energies closer (≈13–18 kcal mol^{-1}) to the experimental values reported for the interaction between adenine and thymine through the bond entalphy (-12.1 kcal mol^{-1}) obtained from mass spectrometry data [45]. Our results are also coherent with other theoretical values for A···T obtained at the MP2 and DFT levels [46–49].

In summary, the results obtained by the semi-extended model are shown to be coherent when the four environments were considered and give a trend for the outside binding, mPy^+ has a slight major affinity for the adenine nucleotide than for the thymine one, accounting for a selectivity degree. In spite of that, it is clear that mPy^+ has an outside binding with the nucleotide pair, and the nucleotide pairs are stabilized by the presence of the cationic species mPy^+.

Extended model

Once we probe the validity of the geometry and interaction energies for the assemblies of the semi-extended model studied with ONIOM, we investigate systems of larger size as cationic porphyrins interacting either with the nucleotide pair adenine-thymine or with guanine-cytosine. The goal of this part of the study is on the first hand to analyze the effect produced by the inclusion of the whole porphyrin on the interaction between bases, and on the second hand to analyze the effect of the size of the cationic substituent that directly interacts with the nucleotide. The semi-extended model was carried out with the aim to explore the reliability of a simple model that could be applied to extended molecular systems.

Figure 6 shows the optimized geometry using three layers ONIOM for the assemblies with interaction by adenine nucleotide and Fig. 7 the corresponding ones by thymine nucleotide. Due to the size of the assemblies, for clarity in the figures we used a tube model instead of ball and stick, tube and frame as correspond to a three layer ONIOM. Basically the interaction with the porphyrin is produced by the formation of H-bonds, which have been specified in the figures and the numerical values are shown in Table 2.

The inclusion of the whole porphyrin in the extended model in comparison with the semi-extended model shows differences in the formation of H-bonds. In the assembly **5,** where the cationic substituent is the same as that in **1**, the same H-bond is formed in outside binding but is larger (2.05 Å) than in **1** (1.98 Å). This indicates that the inclusion of the whole porphyrin in **5** produces a weaker outside binding than in **1**. A similar result occurs with the hydrogen bonding between the base pair, the distance between the hydrogen of the amine in adenine and the oxygen of the carbonyl in thymine is larger (2.41 Å) than in **1** (1.83 Å).

For the extended model, we found an effect of the length of the chain of the cationic substituent. In the case of outside binding, **5** forms two H-bonds and **6** and **7** form three H-bonds with the methyl group that belongs to the cationic substituent. A similar result is obtained with **5′**, **6′** and **7′**. Particularly, we found that in **5** one hydrogen atom in β position of a pyrrolic ring of porphyrin contributes to the formation of H-bond (1.77 Å) with one oxygen atom of the phosphate group. This does not happen in the other assemblies because hydrogen atoms in these structures that participate in the interaction with phosphate group belong to the methyl group that is located away of the porphyrin.

Atomic charge calculations obtained with NPA indicate that H_{84} in **5** is slightly more deficient in charge (q=0.307) than H_{159} (q=0.304) showing that the interaction between the oxygen atom of the phosphate group with the pyrrolic hydrogen (H_{84}) is slightly stronger (Fig. 6). The change of the cationic substituent from methyl pyridyl (**5**) to N-trimethyl aniline (**6**) produces an increase more important in one of the H-bonds of the outside binding from 1.77 to 2.05 Å, and with a similar value when the substituent is three-methyl amine propyl (**7**) (2.08 Å). A similar behavior occurs for the interaction by the thymine nucleotide, a value for H-bond of 1.85 Å for **5′** increases to 2.06 Å (**6′**) and 2.01 Å (**7′**).

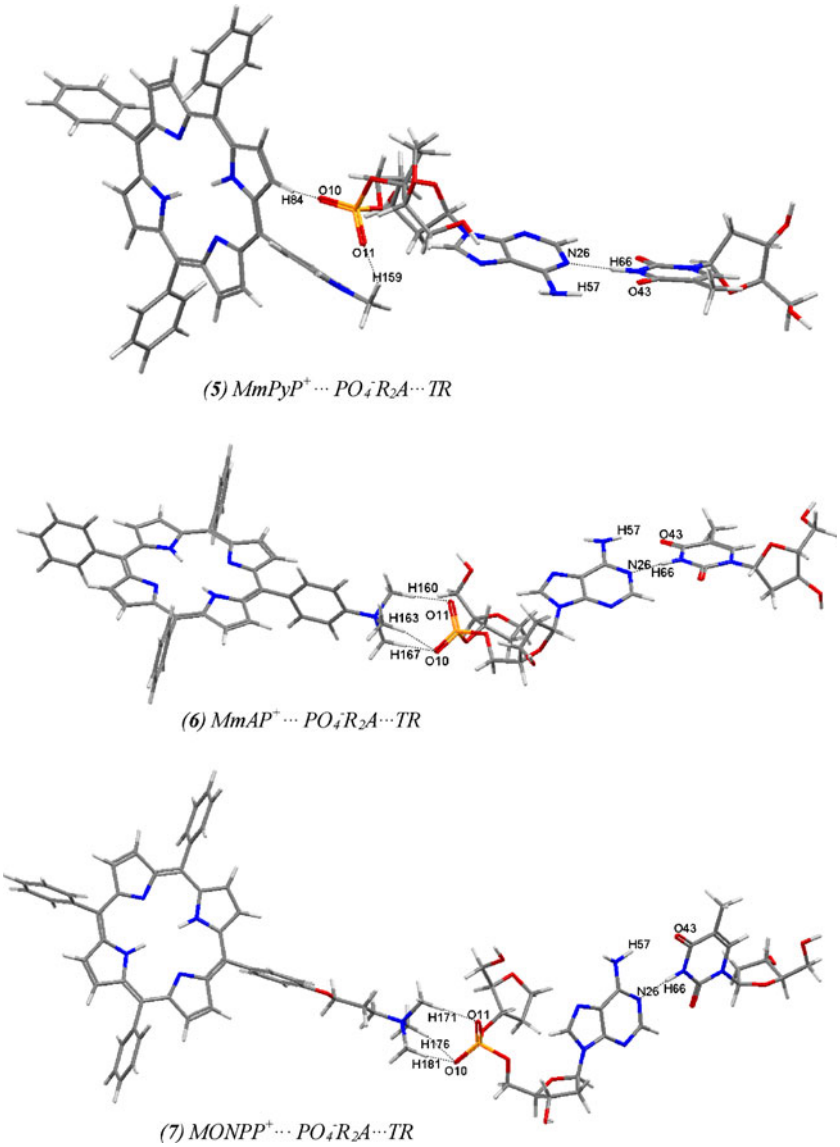

Fig. 6 Optimized molecular assemblies obtained by ONIOM methodology for the extended model, where the outside binding of the cationic porphyrin occurs by the adenine side

In relation to the hydrogen bonding between the base pair, we found that the distance N···H practically is not modified by the change of the substituent (1.79–1.82 Å) and the calculations predict a strong hydrogen bonding in agreement with data reported in the literature for Watson-Crick A···T base pairs (1.7–1.8 Å) [46]. However, the O···H bond undergoes a more important change from 1.81 (**5′**) to 2.38 Å (**6′**, **7′**), suggesting that an increase of the length of the chain in the cationic substituent weakens the interaction between the base pair.

In summary, the presence of the whole porphyrin in an extended model gives account of a slightly weaker interaction for outside binding and for the base pair binding, in comparison with the semi extended model.

In the case of the interaction of porphyrin with the guanine-cytosine nucleotide pair, we observe a favorable interaction with the formation of three strong H-bonds for outside binding. The latter interaction does not modify the affinity between the bases reflected by the formation of three H-bonds, on the contrary, it produces slightly shorter distances for these H-bonds (more details in Fig. 1S).

The interaction energies calculated for outside binding PX···PO_4^- and base pair binding A···T of the assemblies **5-7** and **5′-7′** using the ONIOM geometries are shown in Table 3. In this table the values calculated at the three layers ONIOM level and at B3LYP/6-31G(d,p) level are included. As was obtained for the semi-extended model, we found for both methods of calculation the same trend in the extended model; the interaction by the adenine nucleotide produces more negative values than by the thymine nucleotide and therefore the interaction is more stable for the adenine side. For ONIOM this larger stabilization is ≈7–9 kcalmol^{-1}, and for B3LYP is ≈3–7 kcalmol^{-1}. It suggests that the cationic porphyrins studied are selective for interacting with the nucleotides.

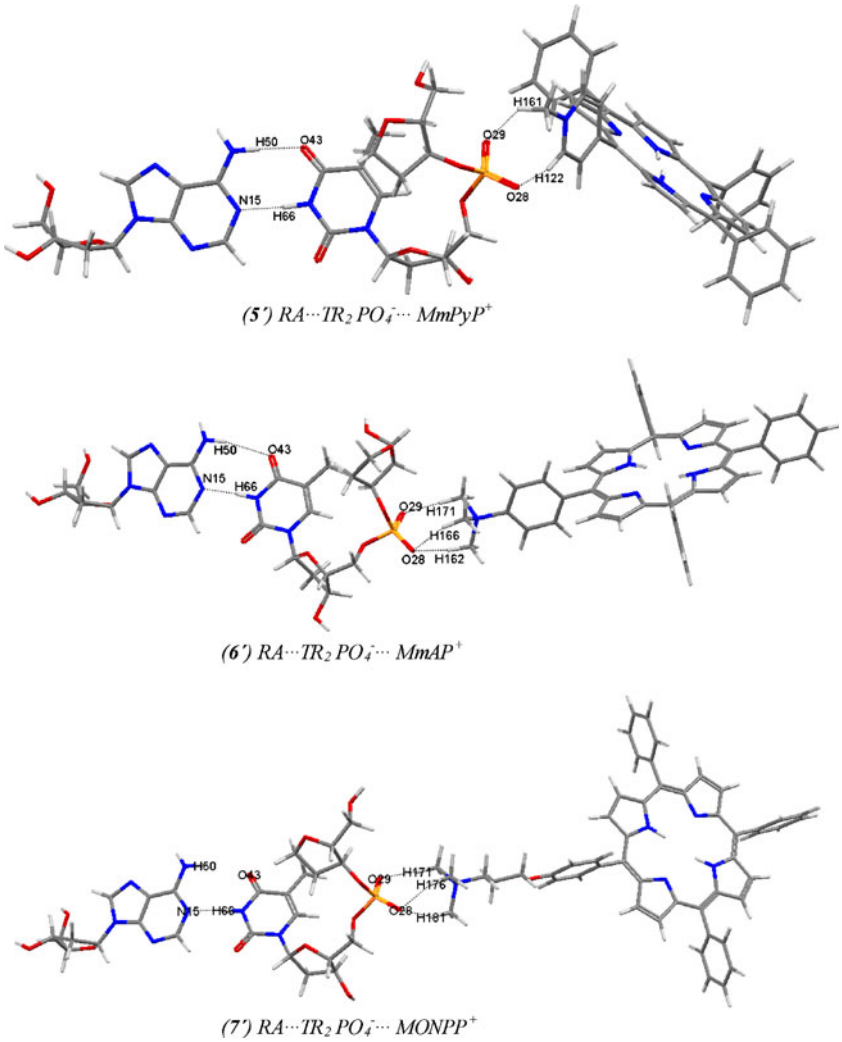

Fig. 7 Optimized molecular assemblies obtained by ONIOM methodology for the extended model, where the outside binding of the cationic porphyrin occurs by the thymine side

Table 2 More relevant distances[a] (Å) for the assemblies obtained with the extended model using the three layers ONIOM model

Interaction by adenine nucleotide					
5: *MmPyP*$^+$··· *PO*$_4^-$*R*$_2$*A*···*TR*		***6***: *MmAP*$^+$··· *PO*$_4^-$*R*$_2$*A*···*TR*		***7***: *MONPP*$^+$··· *PO*$_4^-$*R*$_2$*A*···*TR*	
Outside binding					
H_{84}-O_{10}	1.77	H_{163}-O_{10}	2.05	H_{176}-O_{10}	2.08
H_{159}-O_{11}	2.05	H_{167}-O_{10}	2.04	H_{181}-O_{10}	2.01
		H_{160}-O_{11}	1.93	H_{171}-O_{11}	1.92
A···T					
H_{57}-O_{43}	2.41	H_{57}-O_{43}	2.43	H_{57}-O_{43}	2.43
N_{26}-H_{66}	1.80	N_{26}-H_{66}	1.80	N_{26}-H_{66}	1.80
Interaction by thymine nucleotide					
5′: *RA*···*TR*$_2$ *PO*$_4^-$··· *MmPyP*$^+$		***6′***: *RA*···*TR*$_2$ *PO*$_4^-$··· *MmAP*$^+$		***7′***: *RA*···*TR*$_2$ *PO*$_4^-$··· *MONPP*$^+$	
Outside binding					
H_{122}-O_{28}	1.85	H_{162}-O_{28}	2.06	H_{171}-O_{28}	2.01
H_{161}-O_{29}	2.08	H_{166}-O_{28}	2.03	H_{181}-O_{28}	2.00
		H_{171}-O_{29}	1.93	H_{171}-O_{29}	1.93
A···T					
H_{50}-O_{43}	1.81	H_{50}-O_{43}	2.38	H_{50}-O_{43}	2.38
N_{15}-H_{66}	1.79	N_{15}-H_{66}	1.82	N_{15}-H_{66}	1.82

[a]for numeration see Figs. 6 and 7

Table 3 Interaction energies (E_{int}) for $PX\cdots PO_4^-$ and $A\cdots T$ (kcal mol^{-1}) for the assemblies obtained with the extended model calculated by the three layers ONIOM and B3LYP/6-31G(d,p) over the ONIOM optimized geometries. BSSE errors calculated at the B3LYP/6-31G(d, p) level of theory are included in parenthesis

Interaction by adenine nucleotide	E_{int} $PX\cdots PO_4^-$	$E_{int.}$ $A\cdots T$	Interaction by thymine nucleotide	E_{int} $PX\cdots PO_4^-$	$E_{int.}$ $A\cdots T$
Three layers ONIOM					
PO_4-$R_2A\cdots TR$	-	-4.28	$RA\cdots TR_2PO_4^-$	-	-4.79
5: $MmPyP^+\cdots PO_4^-R_2A\cdots TR$	-96.64	-4.88	***5′***: $RA\cdots TR_2PO_4^-\cdots MmPyP^+$	-87.21	-2.42
6: $MmAP^+\cdots PO_4^-R_2A\cdots TR$	-91.43	-6.51	***6′***: $RA\cdots TR_2PO_4^-\cdots MmAP^+$	-84.08	-3.94
7: $MONPP^+\cdots PO_4^-R_2A\cdots TR$	-98.08	-4.56	***7′***: $RA\cdots TR_2PO_4^-\cdots MONPP^+$	-90.69	-4.79
B3LYP/6-31G(d,p)					
PO_4-$R_2A\cdots TR$	-	-13.58 (4.07)	$RA\cdots TR_2PO_4^-$	-	-15.49 (4.48)
5: $MmPyP^+\cdots PO_4^-R_2A\cdots TR$	-73.53 (7.29)	-16.32 (3.90)	***5′***: $RA\cdots TR_2PO_4^-\cdots MmPyP^+$	-66.99 (4.10)	-13.16 (4.13)
6: $MmAP^+\cdots PO_4^-R_2A\cdots TR$	-77.45 (4.15)	-12.62 (3.92)	***6′***: $RA\cdots TR_2PO_4^-\cdots MmAP^+$	-74.18 (4.25)	-15.99 (4.00)
7: $MONPP^+\cdots PO_4^-R_2A\cdots TR$	-83.33 (4.30)	-14.46 (3.91)	***7′***: $RA\cdots TR_2PO_4^-\cdots MONPP^+$	-79.77 (4.16)	-12.86 (3.96)

In order to verify how well defined the outside binding at B3LYP/6-31G(d,p) level is, means if the level of calculation is enough to describe the electrostatic interaction between mPy^+ and PO_4^-, we did single point calculations for **5** and **5′** over the ONIOM optimized geometries including two sets of diffuse functions (s,p) (B3LYP/6-31++G(d,p)). The diffuse functions predict for both assemblies slightly higher interaction energies (**5**: -68 kcal mol^{-1}; **5′**: -64 kcal mol^{-1}) with respect to the basis set 6-31G(d,p) but a larger stabilization by the adenine side is kept. Hence we choose to continue the study at the B3LYP/6-31G(d,p) level and thus to avoid more computational time that the diffuse functions demand.

On the other hand, we found for both nucleotide sides (Table 3) that the larger chain of the substituent in the porphyrin lowers interaction energy for outside binding, a trend that is more evident for B3LYP calculations. These results show a way to modulate the bonding porphyrin···DNA to account later in photodynamical processes.

In relation to the interaction between the bases adenine···thymine, the semiempirical PM3 level used in the ONIOM calculations predicts interaction energies of ≈-4 to -6 kcal mol^{-1} for two hydrogen bonding (including or not the porphyrin) that is not in agreement with theoretical values reported for RI-MP2/aug-cc-pVDZ (-13.8 kcal mol^{-1}) and RI-MP2/aug-cc-pVTZ (-14.7 kcal mol^{-1}) [50] and bond enthalpies (-12.1 kcal mol^{-1}) [45]. Note that B3LYP calculations (Table 3) predict values of -13.6 and -15.5 kcal mol^{-1} for that interaction without porphyrin depending on the model used for outside binding (two ribose rings and one phosphate group). The inclusion of porphyrin produces a slight stabilization (**5**, **7**, **6`**) and unstabilization (**6**, **5`**, **7`**) of the adenine···thymine interaction of ≈1–2 kcal mol^{-1}.

For the interaction between porphyrin and the guanine-cytosine nucleotide pair, the same theoretical methods as used in adenine-thymine assemblies are applied and the results of interaction energies are presented in Table 4. We found that both outside bindings, by guanine or cytosine

Table 4 Interaction energies (E_{int}) for $PX\cdots PO_4^-$ and $G\cdots C$ (kcal mol^{-1}) for the assemblies obtained with the extended model calculated by the three layers ONIOM and B3LYP/6-31G(d,p) over the ONIOM optimized geometries. BSSE errors calculated at the B3LYP/6-31G(d, p) level of theory are included in parenthesis

Interaction by guanine nucleotide	E_{int} $PX\cdots PO_4^-$	$E_{int.}$ $G\cdots C$	Interaction by cytosine nucleotide	E_{int} $PX\cdots PO_4^-$	$E_{int.}$ $G\cdots C$
Three layers ONIOM					
$PO_4^-R_2G\cdots CR$	-	-9.83	$RG\cdots CR_2PO_4^-$	-	-15.27
8: $MmPyP^+\cdots PO_4^-R_2G\cdots CR$	-94.75	-11.13	***8′***: $RG\cdots CR_2PO_4^-\cdots MmPyP^+$	-85.83	-12.92
9: $MmAP^+\cdots PO_4^-R_2G\cdots CR$	-91.01	-11.25	***9′***: $RG\cdots CR_2PO_4^-\cdots MmAP^+$	-85.60	-14.92
10: $MONPP^+\cdots PO_4^-R_2G\cdots CR$	-97.21	-8.25	***10′***: $RG\cdots CR_2PO_4^-\cdots MONPP^+$	-91.24	-13.66
B3LYP/6-31G(d,p)					
$PO_4^-R_2G\cdots CR$	-	-28.78 (4.97)	$RG\cdots CR_2PO_4^-$	-	-36.12 (5.18)
8: $MmPyP^+\cdots PO_4^-R_2G\cdots CR$	-70.15 (6.76)	-24.47 (4.78)	***8′***: $RG\cdots CR_2PO_4^-\cdots MmPyP^+$	-61.50 (6.84)	-31.95 (4.92)
9: $MmAP^+\cdots PO_4^-R_2G\cdots CR$	-76.89 (4.61)	-29.62 (4.78)	***9′***: $RG\cdots CR_2PO_4^-\cdots MmAP^+$	-65.85 (3.87)	-25.25 (4.92)
10: $MONPP^+\cdots PO_4^-R_2G\cdots CR$	-82.33 (4.18)	-24.23 (4.75)	***10′***: $RG\cdots CR_2PO_4^-\cdots MONPP^+$	-73.93 (3.85)	-27.23 (4.89)

nucleotide, are favored (negative interaction energies) and a similar trend is found for ONIOM and B3LYP, the interaction of porphyrin by guanine nucleotide is preferred by 6–9 kcalmol^{-1} in ONIOM and by 8–11 kcalmol^{-1} in B3LYP over the interaction that occurs by cytosine nucleotide. We again obtained lower interaction energies of outside binding for the three layers ONIOM compared with B3LYP.

The interaction between the base pair G···C shows more negative values for B3LYP than ONIOM accounting for the formation of three H-bonds in agreement with that found by Sponer et al. [50] at the levels of theory RI-MP2/aug-cc-pVDZ (-25.6 kcalmol^{-1}) and RI-MP2/aug-cc-pVTZ (-27.0 kcalmol^{-1}). In ONIOM we used the semiempirical PM3 method that is unable to predict the correct values for that interaction. However, B3LYP predicts values in agreement with theoretical data reported (-26 to -28 kcalmol^{-1} [46]; -23.8 kcalmol^{-1} [48]; -26.1 kcalmol^{-1} [47]; -25 kcal mol^{-1} [49]) and bond enthalpies (-21 kcalmol^{-1}) [45].

The interaction between the bases C···G is favored when the porphyrin is approached to the cytosine nucleotide compared to the guanine nucleotide, which is coherent with a lower affinity of outside binding.

In order to investigate the basis set superposition error (BSSE) associated to the calculation of the interaction energy (outside binding and hydrogen bonding), we used the counterpoise method proposed by Boys and Bernardi to correct these energies and the errors obtained at the B3LYP level are included in Tables 3 and 4 in parenthesis [51]. Overall for adenine-thymine and guanine-cytosine assemblies the BSSE errors are of 5–10 % for outside binding and 15–31 % for hydrogen bonding between base pairs being a little smaller for the latter assemblies. Although the magnitude of the errors is very similar (≈4 kcal mol^{-1}) it represents a more important error for the description of the hydrogen bonding between base pairs. These results suggest that B3LYP/6-31G(d,p) is not enough for that description and a more sophisticated theoretical method is required.

In summary, we found that the interaction of a porphyrin with a nucleotide by the mode of outside binding is numerically different for the set of bases studied and that interaction is favored in the following order: adenine > guanine > thymine > cytosine. However, the differences obtained between them are not more than ≈10 kcal mol^{-1} which are not significant for the size of the molecular assembly, suggesting that the porphyrin could interact with whichever of the base pairs in the DNA environment.

Conclusions

We performed a systematic study to investigate at a molecular level the outside binding mode of a cationic porphyrin and a nucleotide pair of adenine-thymine and guanine-cytosine forming a supramolecular assembly. In order to do that, we used two structural models (semi-extended, extended) that differ in the size of the porphyrins, which were calculated under two kinds of theoretical methods: quantum mechanics molecular mechanics given by a three layer ONIOM (B3LYP/6-31G(d)/PM3/UFF) and only quantum mechanics given by B3LYP/6-31G(d,p). We investigated several effects: (a) the environment in the semi-extended model; gas phase, solution phase using an explicit solvent model (H_2O), in the presence of a sodium cation (Na^+) and in both (H_2O + Na^+), (b) the type of nucleotide in the extended model; adenine-thymine and guanine-cytosine nucleotides, and (c) the chain length of the cationic substituent in the porphyrin.

For the semi-extended and extended models we found a trend in the outside binding, the interaction energy calculated by ONIOM and B3LYP/6-31G(d,p) shows a preference of the cationic substituent for binding to adenine nucleotide by ≈6-23 kcalmol^{-1} over thymine. The binding between the base pair in the nucleotides is stabilized when the interaction with the cationic porphyrin is produced, denoting that the outside binding is a favorable interaction. The extended model showed that the affinity of these cationic porphyrin by the nucleotides follows the order: adenine > guanine > thymine > cytosine, and the differences between these interaction energies are not longer than 10 kcalmol^{-1} suggesting that this kind of cationic porphyrin presents a little selectivity toward the nucleotides.

Acknowledgments The authors thank FONDECYT N°1090700 (CONICYT/CHILE) for financial support and DICYT/USACH Apoyo Complementario for computational time provided. LCS thanks CONICYT for doctoral fellowship.

References

1. Gibbs EJ, Tinoco JI, Maestre MF, Ellinas PA, Pasternack RF (1988) Self-assembly of porphyrins on nucleic acid templates. Biochem Bioph Res Co 157(1):350–358. doi:10.1016/s0006-291x(88)80054-8
2. Lang K, Mosinger J, Wagnerová DM (2004) Photophysical properties of porphyrinoid sensitizers non-covalently bound to host molecules; models for photodynamic therapy. Coord Chem Rev 248(3–4):321–350. doi:10.1016/j.ccr.2004.02.004
3. McMillin DR, Shelton AH, Bejune SA, Fanwick PE, Wall RK (2005) Understanding binding interactions of cationic porphyrins with B-form DNA. Coord Chem Rev 249(13–14):1451–1459. doi:10.1016/j.ccr.2004.11.016
4. Munson BR, Fiel RJ (1992) DNA intercalation and photosensitization by cationic meso substituted porphyrins. Nucl Acids Res 20 (6):1315–1319
5. Okada H, Imai H, Uemori Y (2001) Intercalation of water-soluble bis-Porphyrins into Poly(dA)-Poly(dT) double helix. Bioorg Med Chem 9(12):3301–3307. doi:10.1016/s0968-0896(01)00239-5

6. Pasternack RF, Gibbs EJ (1983) Porphyrin interactions with nucleic acids. Inorg Chim Acta 79:7–7. doi:10.1016/s0020-1693(00)95023-0
7. Vicente MGH (2001) Porphyrin-based sensitizers in the detection and treatment of cancer: recent progress. Curr Med Chem Anti-Cancer Agents 1:175–194. doi:10.2174/1568011013354769
8. Zheng YM, Wang K, Li T, Zhang XL, Li ZY (2011) Synthesis, singlet oxygen photogeneration and DNA photo-cleavage of porphyrins with nitrogen heterocycle tails. Molecules 16(5):3488–3498
9. Manono J, Marzilli PA, Marzilli LG (2009) New porphyrins bearing positively charged peripheral groups linked by a sulfonamide group to meso-tetraphenylporphyrin: interactions with calf thymus DNA. Inorg Chem 48(13):5636–5647. doi:10.1021/ic900385y
10. Vedachalam S, Choi BH, Pasunooti KK, Ching KM, Lee K, Yoon HS, Liu XW (2011) Glycosylated porphyrin derivatives and their photodynamic activity in cancer cells. Med Chem Comm 2 (5):371–377
11. Mező G, Herényi L, Habdas J, Majer Z, Myśliwa-Kurdziel B, Tóth K, Csík G (2011) Syntheses and DNA binding of new cationic porphyrin–tetrapeptide conjugates. Biophys Chem 155(1):36–44. doi:10.1016/j.bpc.2011.02.007
12. Fiel RJ, Howard JC, Mark EH, Gupta ND (1979) Interaction of DNA with a porphyrin ligand: evidence for intercalation. Nucleic Acids Res 6(9):3093–3118. doi:10.1093/nar/6.9.3093
13. Tabata M, Nakajima K, Nyarko E (2000) Metalloporphyrin mediated DNA cleavage by a low concentration of HaeIII restriction enzyme. J Inorg Biochem 78(4):383–389. doi:10.1016/s0162-0134(00)00067-2
14. Zhao P, Huang JW, Mei WJ, He J, Ji LN (2010) DNA binding and photocleavage specificities of a group of tricationic metalloporphyrins. Spectrochim Acta A Mol Biomol Spectrosc 75(3):1108–1114. doi:10.1016/j.saa.2009.12.065
15. Carvlin MJ, Mark E, Fiel R, Howard JC (1983) Intercalative and nonintercalative binding of large cationic porphyrin ligands to polynucleotides. Nucleic Acids Res 11(17):6141–6154. doi:10.1093/nar/11.17.6141
16. Carvlin MJ, Fiel RJ (1983) Intercalative and nonintercalative binding of large cationic porphyrin ligands to calf thymus DNA. Nucleic Acids Res 11(17):6121–6139. doi:10.1093/nar/11.17.6121
17. Biver T, Secco F, Venturini M (2008) Mechanistic aspects of the interaction of intercalating metal complexes with nucleic acids. Coord Chem Rev 252(10–11):1163–1177. doi:10.1016/j.ccr.2007.10.008
18. Pasternack RF, Brigandi RA, Abrams MJ, Williams AP, Gibbs EJ (1990) Interactions of porphyrins and metalloporphyrins with single-stranded poly(dA). Inorg Chem 29(22):4483–4486. doi:10.1021/ic00347a030
19. Pasternack RF, Gibbs EJ, Villafranca JJ (1983) Interactions of porphyrins with nucleic acids. Biochemistry 22(10):2406–2414. doi:10.1021/bi00279a016
20. Strickland JA, Marzilli LG, Wilson WD, Zon G (1989) Metalloporphyrin DNA interactions: insights from NMR studies of oligodeoxyribonucleotides. Inorg Chem 28(23):4191–4198. doi:10.1021/ic00322a005
21. Ward B, Skorobogaty A, Dabrowiak JC (1986) DNA binding specificity of a series of cationic metalloporphyrin complexes. Biochemistry 25(24):7827–7833. doi:10.1021/bi00372a007
22. Marzilli LG, Petho G, Lin M, Kim MS, Dixon DW (1992) Tentacle porphyrins: DNA interactions. J Am Chem Soc 114 (19):7575–7577. doi:10.1021/ja00045a047
23. Mukundan NE, Petho G, Dixon DW, Kim MS, Marzilli LG (1994) Interactions of an electron-rich tetracationic tentacle porphyrin with calf thymus DNA. Inorg Chem 33(21):4676–4687. doi:10.1021/ic00099a018
24. McClure JE, Baudouin L, Mansuy D, Marzilli LG (1997) Interactions of DNA with a new electron-deficient tentacle porphyrin: meso-Tetrakis[2,3,5,6-tetrafluoro-4-(2-trimethylammoniumethylamine)phenyl]porphyrin. Biopolymers 42(2):203–217. doi:10.1002/(sici)1097-0282(199708)42:2<203::aid-bip9>3.0.co;2-r
25. Wu S, Li Z, Ren L, Chen B, Liang F, Zhou X, Jia T, Cao X (2006) Dicationic pyridium porphyrins appending different peripheral substituents: Synthesis and studies for their interactions with DNA. Bioorg Med Chem 14(9):2956–2965. doi:10.1016/j.bmc.2005.12.011
26. Svensson M, Humbel S, Froese RDJ, Matsubara T, Sieber S, Morokuma K (1996) ONIOM: a multilayered integrated MO + MM method for geometry optimizations and single point energy predictions. A test for diels − alder reactions and Pt(P(t-Bu)3)2 + H2 oxidative addition. J Phys Chem 100(50):19357–19363. doi:10.1021/jp962071j
27. Humbel S, Sieber S, Morokuma K (1996) The IMOMO method: integration of different levels of molecular orbital approximations for geometry optimization of large systems: test for n-butane conformation and S[sub N]2 reaction: RCl + Cl[sup -]. J Chem Phys 105(5):1959–1967
28. Dapprich S, Komáromi I, Byun KS, Morokuma K, Frisch MJ (1999) A new ONIOM implementation in Gaussian98. Part I. The calculation of energies, gradients, vibrational frequencies and electric field derivatives. J Mol Struct (THEOCHEM) 461-462:1–21. doi:10.1016/s0166-1280(98)00475-8
29. Tschumper GS, Morokuma K (2002) Gauging the applicability of ONIOM (MO/MO) methods to weak chemical interactions in large systems: hydrogen bonding in alcohol dimers. J Mol Struct (THEOCHEM) 592(1–3):137–147. doi:10.1016/s0166-1280(02)00234-8
30. Re S, Morokuma K (2001) ONIOM study of chemical reactions in microsolvation clusters: (H2O)nCH3Cl + OH-(H2O)m (n+m=1 and 2). J Phys Chem A 105(30):7185–7197. doi:10.1021/jp004623a
31. Ruiz R, García B, Ruisi G, Silvestri A, Barone G (2009) Computational study of the interaction of proflavine with d(ATATATATAT)2 and d(GCGCGCGCGC)2. J Mol Struct (THEOCHEM) 915(1–3):86–92. doi:10.1016/j.theochem.2009.08.022
32. Ahmadi F, Jamali N, Jahangard-Yekta S, Jafari B, Nouri S, Najafi F, Rahimi-Nasrabadi M (2011) The experimental and theoretical QM/MM study of interaction of chloridazon herbicide with ds-DNA. Spectrochim Acta A Mol Biomol Spectrosc 79(5):1004–1012. doi:10.1016/j.saa.2011.04.012
33. Banik SD, Nandi N (2009) Orientation and distance dependent chiral discrimination in the first step of the aminoacylation reaction: Integrated molecular orbital and semi-empirical method (ONIOM) based calculation. Colloids Surf B 74(2):468–476. doi:10.1016/j.colsurfb.2009.07.019
34. Chen HY, Kao CL, Hsu SCN (2009) Proton transfer in guanine − cytosine radical anion embedded in B-form DNA. J Am Chem Soc 131(43):15930–15938. doi:10.1021/ja906899p
35. Becke AD (1988) Density-functional exchange-energy approximation with correct asymptotic behavior. Phys Rev A 38(6):3098–3100
36. Becke AD (1993) Density-functional thermochemistry. III. The role of exact exchange. J Chem Phys 98(7):5648–5652
37. Lee C, Yang W, Parr RG (1988) Development of the Colle-Salvetti correlation-energy formula into a functional of the electron density. Phys Rev B 37(2):785–789
38. Stewart JJP (1989) Optimization of parameters for semiempirical methods I. Method. J Comput Chem 10(2):209–220. doi:10.1002/jcc.540100208
39. Sundaresan N, Suresh CH (2007) A base-sugar − phosphate three-layer ONIOM model for cation binding: relative binding affinities

of alkali metal ions for phosphate anion in DNA. J Chem Theor Comput 3(3):1172–1182. doi:10.1021/ct600245w
40. Sundaresan N, Pillai CKS, Suresh CH (2006) Role of Mg2+ and Ca2+ in DNA bending: evidence from an ONIOM-based QM-MM study of a DNA fragment. J Phys Chem A 110(28):8826–8831. doi:10.1021/jp061774q
41. Rappe AK, Casewit CJ, Colwell KS, Goddard WA, Skiff WM (1992) UFF, a full periodic table force field for molecular mechanics and molecular dynamics simulations. J Am Chem Soc 114 (25):10024–10035. doi:10.1021/ja00051a040
42. Reed AE, Weinhold F (1983) Natural bond orbital analysis of near-Hartree–Fock water dimer. J Chem Phys 78(6):4066–4073
43. Reed AE, Weinstock RB, Weinhold F (1985) Natural population analysis@f[sup a]@f[sup)]. J Chem Phys 83(2):735–746
44. Frisch MJ, Trucks GW, Schlegel HB, Scuseria GE, Robb MA, Cheeseman JR, Montgomery JA, Vreven JT, Kudin KN, Burant JC, Millam JM, Iyengar SS, Tomasi J, Barone V, Mennucci B, Cossi M, Scalmani G, Rega N, Petersson GA, Nakatsuji H, Hada M, Ehara M, Toyota K, Fukuda R, Hasegawa J, Ishida M, Nakajima T, Honda Y, Kitao O, Nakai H, Klene M, Li X, Knox JE, Hratchian HP, Cross JB, Bakken V, Adamo C, Jaramillo J, Gomperts R, Stratmann RE, Yazyev O, Austin AJ, Cammi R, Pomelli C, Ochterski JW, Ayala PY, Morokuma K, Voth GA, Salvador P, Dannenberg JJ, Zakrzewski VG, Dapprich S, Daniels AD, Strain MC, Farkas O, Malick DK, Rabuck AD, Raghavachari K, Foresman JB, Ortiz JV, Cui Q, Baboul AG, Clifford S, Cioslowski J, Stefanov BB, Liu G, Liashenko A, Piskorz P, Komaromi I, Martin RL, Fox DJ, Keith T, Al-Laham MA, Peng CY, Nanayakkara A, Challacombe M, Gill PMW, Johnson B, Chen W, Wong MW, Gonzalez C, Pople JA (2007) Gaussian 03, Revision E.01. Wallingford, CT
45. Yanson IK, Teplitsky AB, Sukhodub LF (1979) Experimental studies of molecular interactions between nitrogen bases of nucleic acids. Biopolymers 18(5):1149–1170. doi:10.1002/bip.1979.360180510
46. Fonseca Guerra C, Bickelhaupt FM, Snijders JG, Baerends EJ (2000) Hydrogen bonding in DNA base pairs: reconciliation of theory and experiment. J Am Chem Soc 122(17):4117–4128. doi:10.1021/ja993262d
47. Fonseca Guerra C, Bickelhaupt FM, Baerends EJ (2002) Orbital interactions in hydrogen bonds important for cohesion in molecular crystals and mismatched pairs of DNA bases. Cryst Growth Des 2(3):239–245. doi:10.1021/cg010034y
48. Šponer J, Leszczynski J, Hobza P (1996) Structures and energies of hydrogen-bonded DNA base pairs. A nonempirical study with inclusion of electron correlation. J Phys Chem 100(5):1965–1974. doi:10.1021/jp952760f
49. Kurita N, Danilov VI, Anisimov VM (2005) The structure of Watson–Crick DNA base pairs obtained by MP2 optimization. Chem Phys Lett 404(1–3):164–170. doi:10.1016/j.cplett.2005.01.087
50. Šponer J, Jurečka P, Hobza P (2004) Accurate interaction energies of hydrogen-bonded nucleic acid base pairs. J Am Chem Soc 126 (32):10142–10151. doi:10.1021/ja048436s
51. Boys SF, Bernardi F (1970) The calculation of small molecular interactions by the differences of separate total energies. Some procedures with reduced errors. Mol Phys 19(4):553–566. doi:10.1080/00268977000101561